



*J. Serb. Chem. Soc.* 80 (9) 1139–1148 (2015)  
JSCS–4786

## Theoretical study on the Diels–Alder reaction of bromo-substituted 2*H*-pyran-2-ones and some substituent vinyls

MINA HAGHDADI\*, HAMED AMANI and NASIM NAB

*Department of Chemistry, Islamic Azad University, P. O. Box 755, Babol branch, Babol, Iran*

(Received 5 December 2014, revised 8 February, accepted 8 February 2015)

**Abstract:** A DFT study of the reactivity, regio- and stereoselectivity of Diels–Alder reactions between 3-bromo, 5-bromo, and 3,5-dibromo-2*H*-pyran-2-ones and some weakly activated and unactivated alkenes was performed using the density functional theory (DFT). Four possible reaction channels, which are related to the formation of *meta*- and *para*- and *endo*- and *exo*-cycloadducts, were explored and characterized. The energy and natural bond orbital analysis showed that the *meta*-regioselectivity on the *exo* pathway was preferred and followed an asynchronous concerted mechanism with a polar nature in all Diels–Alder cycloadditions. Moreover, the activation free energies of the Diels–Alder cycloadditions of 3,5-dibromo-2*H*-pyran-2-one were lower than those for 3-bromo-2*H*-pyran-2-one and 5-bromo-2*H*-pyran-2-one, which is in line with experimental observations. DFT-based reactivity indices clearly predicted the regiochemistry of the isolated cycloadducts.

**Keywords:** bromo-2*H*-pyran-2-ones; DFT study; reaction mechanism; reactivity indices; regio- and stereoselectivity.

### INTRODUCTION

During investigations on the role of substituents on the cycloaddition reaction of 2*H*-pyran-2-ones, it was found that 3-bromo and 5-bromo-2*H*-pyran-2-ones are the most interesting and unique, and have useful features.<sup>1–5</sup> These two 2*H*-pyran-2-ones are ambident dienes<sup>3</sup> and react with electron-rich, electron-poor and electron-neutral dienophiles with good regio- and stereoselectivity.<sup>4,6,7</sup> The cycloadditions of 2*H*-pyran-2-one itself are not selective.<sup>5</sup> Moreover, in contrast to the bromo-pyrones, 4-chloro-2*H*-pyran-2-one, in line with 2*H*-pyran-2-one itself, is neither ambident diene nor undergoes regioselective cycloadditions.<sup>8</sup> It undergoes cycloadditions only with electron-deficient dienophiles that were stereoselective, but not regioselective.<sup>3a</sup> During the course of a study of 2*H*-

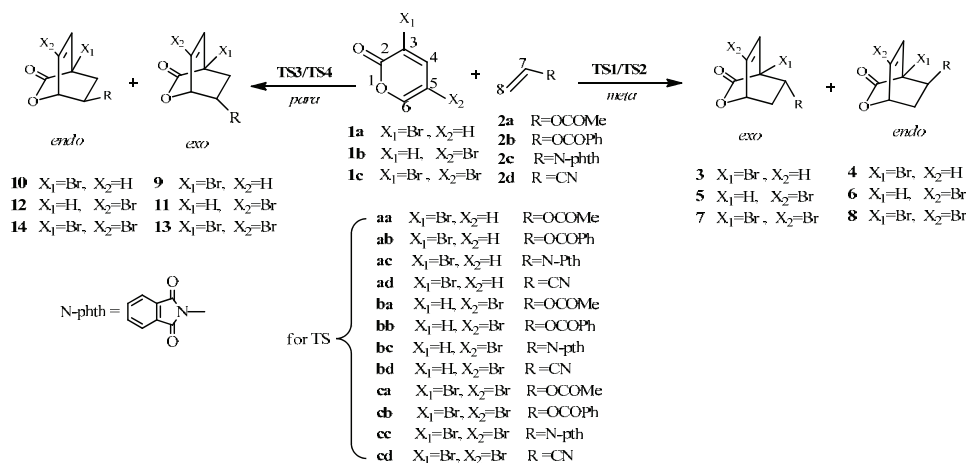
\* Corresponding author. E-mail: mhaghdadi2@gmail.com  
doi: 10.2298/JSC141205014H

-pyran-2-ones, Cho and co-workers investigated 3,5-dibromo-2*H*-pyran-2-one in Diels–Alder (DA) reactions with a series of electronically and sterically distinct dienophiles.<sup>3b</sup> Their results showed that it is a highly potent ambident diene, being more reactive and stereoselective than monobromo-2*H*-pyran-2-ones, and thus capable of generating a variety of bicycloadducts in much higher chemical yields and *endo/exo* ratios than monobromo-2*H*-pyran-2-ones.<sup>3</sup>

Afarinkia and co-workers studied the Diels–Alder reactions of 3- and 5-halo-substituted 2*H*-pyran-2-ones with poor electron-rich, electron-rich and deficient dienophiles.<sup>7–9</sup> Their experimental results showed that these cycloadditions proceed with excellent regioselectivity and very good stereoselectivity. In contrast, the 4-halo-substituted-2*H*-pyran-2-ones reactions proceed with only moderate regio- and stereoselectivity.<sup>9</sup> Furthermore, their results showed that the nature of halogen substituent had only a small, sometimes negligible, influence on the cycloaddition of 2*H*-pyran-2-ones, and also, in both the 3- and 5-substituted series, the distribution of the products did not appear to be significantly different.<sup>8</sup> Therefore, changing the halogen substituent did not significantly change the electronic demand of the 3- and 5-halo-substituted 2*H*-pyran-2-one, although it may influence their reactivity. Furthermore, they performed a range of calculations on substituted 2*H*-pyran-2-one cyclo-additions, at the B3LYP/6-31G level of theory, to demonstrate the advantage of 3- and 5-halo-substituted 2*H*-pyran-2-ones over 4-halo-substituted 2*H*-pyran-2-ones.<sup>8,9</sup>

Although there are many reports about the alternative synthetic routes,<sup>3–9</sup> there are no theoretical investigations about the detailed molecular mechanism and electronic parameters. As a part of a program directed toward the investigation of related DA cycloadditions, herein the results of a theoretical study on the mechanism of cycloaddition reactions between 3-bromo, 5-bromo and 3,5-dibromo-2*H*-pyran-2-ones **1a–c**, with a range of vinyl derivatives: vinyl acetate (**2a**), vinyl benzoate (**2b**), 2-ethenyl-1*H*-isoindole-1,3(2*H*)-dione (*N*-vinylphthalimide) (**2c**) and 2-propenenitrile (**2d**), to give the bridged bicyclic lactones **3–13** are presented (Scheme 1). The purpose of the present study was to provide a better understanding the mechanistic features of these processes, especially by localization and characterization of all stationary points involved in these formally [2+4]cycloadditions. A density functional theory (DFT) analysis was performed to explain both the *exo/endo* stereocontrol and regioselectivity of these processes in order to find a possible mechanism that may explain the different reactivity observed in each case.

Although DA cycloadditions of 5-bromo and 3,5-dibromo-2*H*-pyran-2-ones with poor electron-rich dienophiles **2a–c** were not prepared as part of experimental studies, the calculations based on them provided a better understanding of the trends, differences, and similarities between halogen substituted 2*H*-pyran-2-ones.



Scheme 1. The calculated possible reaction channels for the DA reaction of bromo-substituted 2H-pyran-2-ones **1a–c** with the vinyl derivatives **2a–d** at the B3LYP/cc-pVDZ level.

#### COMPUTATIONAL DETAILS

The density functional theory calculations were realized using the Gaussian 09 package.<sup>10</sup> The relative energies and free energies were computed at 298 K for the various stationary points at the B3LYP/cc-pVDZ level. The electronic structures of the stationary points were analyzed by the natural bond orbital (NBO) method.<sup>11</sup> The global reactivity indexes were estimated according to the equations recommended by Parr.<sup>12</sup> The global electrophilicity index,  $\omega$ , is given by the following expression:<sup>13</sup>

$$\omega = \frac{\mu^2}{2\eta} \quad (1)$$

in terms of the electronic chemical potential,  $\mu$ , and the chemical hardness,  $\eta$ . Both quantities may be approached in terms of the one-electron energies of the frontier molecular orbitals HOMO and LUMO,  $\varepsilon_{\text{H}}$  and  $\varepsilon_{\text{L}}$ ,<sup>14</sup> as:

$$\mu = (\varepsilon_{\text{H}} + \varepsilon_{\text{L}}) / 2 \quad (2)$$

$$\eta = \varepsilon_{\text{L}} - \varepsilon_{\text{H}} \quad (3)$$

Recently, Domingo introduced an empirical (relative) nucleophilicity index,  $N$ ,<sup>15</sup> based on the HOMO energies obtained within the Kohn Sham scheme,<sup>13</sup> and defined as:

$$\varepsilon_{\text{HOMO}}(\text{Nu}) - \varepsilon_{\text{HOMO}}(\text{TCE}) \quad (4)$$

Nucleophilicity is referred to tetracyanoethylene (TCE), because it presents the lowest HOMO energy in a large series of molecules already investigated within the context of polar cycloadditions. This choice allows the convenient handling of a nucleophilicity scale of positive values. Recently, Domingo proposed two new electrophilic,  $P_k^+$ , and nucleophilic,  $P_k^-$ , Parr functions based on the atomic spin density distribution at the radical anion and cation of a neutral molecule.<sup>16</sup> The electrophilic,  $P_k^+$ , and nucleophilic,  $P_k^-$ , Parr functions, were obtained through the analysis of the Mulliken atomic spin density of the radical anion and cation by single-point energy calculations over the optimized neutral geometries using the

unrestricted UB3LYP formalism for radical species. The local electrophilicity indices,  $\omega_k$ ,<sup>17</sup> the local nucleophilicity indices,  $N_k$ ,<sup>198</sup> were calculated using the following expressions:

$$\omega_k = \omega P_k^+ \quad (5)$$

$$N_k = N P_k^- \quad (6)$$

where  $P_k^+$  and  $P_k^-$  are the electrophilic and nucleophilic Parr functions,<sup>16</sup> respectively.

## RESULTS AND DISCUSSIONS

In the present study, the regio- and stereoselectivity of the cycloaddition reaction between bromo-substituted 2*H*-pyran-2-ones **1a–c** and vinyl substituents **2a–d** were studied, and then an analysis based on the reactivity indices of stationary points was performed.

### *Study of the DA reactions of bromo-substituted 2H-pyran-2-ones 1a–c with some vinyl derivatives (2a–d)*

Due to the asymmetry of bromo-substituted 2*H*-pyran-2-ones **1a–c**, four regio-isomeric channels are feasible for each of the DA reactions, *meta* and *para*, which are related to the *endo* and *exo* approach modes of the diene systems **1a–c** relative to the R group of the vinyl compounds **2a–d** (Scheme 1).

Analysis of the stationary points associated with these DA reactions indicated that they could occur *via* a one-step mechanism and consequently, four stereoisomeric TSs, named **TS1**, **TS2**, **TS3**, and **TS4**, and the corresponding products **3–13** were located and characterized. The activation and relative energies associated with these stationary points are given in Table I. Analysis of the geometries at the **TS** structures shows that the **TSs** of *meta* pathways correspond to asynchronous bond formation processes. The extent of bond formation along a reaction pathway is provided by the concept of bond order (BO).<sup>19</sup> These values are within the range of 0.180 to 0.636. These results show that for all DA reactions, **TS1** and **TS2** (*meta* pathways) are more asynchronous than **TS3** and **TS4** (*para* pathways), and that the **TSc<sub>a</sub>**, **TSc<sub>b</sub>** and **TSc<sub>c</sub>** (for the *N*-phthalimide substituent) are the most asynchronous ones. The asynchronicity shown by the geometrical data is accounted for by the BO values.

Furthermore, the asynchronicity in bond formation at the **TSs** measured by  $\Delta r = (r_2 - r_1)$  ranges from 0.72 to 1.10 at **TS1** and **TS2**, indicating that the **TSs** of *meta* process correspond to highly asynchronous bond-formation processes. Natural population analysis (NPA)<sup>11</sup> allowed the evaluation of the charge transfer (CT) along these DA reactions, at the **TSs**. Charge transfer (CT) plays a relevant role in most of organic reactions. In fact, in Diels–Alder reactions, the *CT* value is one of the most relevant characteristics of their transition states (**TSs**) and, in most cases, it is responsible of the height of their energy barrier. The calculated *CT* values for these DA reactions are given in Fig. 1. In general, the *CT* values in the **TSs** associated with the *para* pathways were lower than 0.090 e, in clear agree-

TABLE I. Activation energies,  $\Delta E^\ddagger$ , activation free energies,  $\Delta G^\ddagger$ , and reaction energies,  $\Delta E_r$ , (all in  $\text{kJ mol}^{-1}$ ), with the formation of DA cycloadducts between bromo-substituted 2H-pyran-2-ones **1a–c** and vinyl derivatives **2a–d** in the *meta* pathways

Entry	Species	TS	$\Delta E^\ddagger$	$\Delta G^\ddagger$	$\Delta E_r$
1	<b>1a+2a</b> → <b>3a-exo</b>	<b>TS1aa</b>	108.48	166.33	-48.53
2	<b>1a+2a</b> → <b>4a-endo</b>	<b>TS2aa</b>	112.94	169.31	-46.22
3	<b>1a+2b</b> → <b>3b-exo</b>	<b>TS1ab</b>	112.12	168.26	-49.94
4	<b>1a+2b</b> → <b>4b-endo</b>	<b>TS2ab</b>	116.66	170.56	-45.98
5	<b>1a+2c</b> → <b>3c-exo</b>	<b>TS1ac</b>	106.75	163.59	-28.80
6	<b>1a+2c</b> → <b>4c-endo</b>	<b>TS2ac</b>	112.64	168.23	-27.73
7	<b>1a+2d</b> → <b>3d-exo</b>	<b>TS1ad</b>	117.59	171.64	-29.45
8	<b>1a+2d</b> → <b>4d-endo</b>	<b>TS2ad</b>	107.65	161.71	-33.67
9	<b>1b+2a</b> → <b>5a-exo</b>	<b>TS1ba</b>	92.82	150.75	-69.94
10	<b>1b+2a</b> → <b>6a-endo</b>	<b>TS2ba</b>	102.04	157.18	-65.45
11	<b>1b+2b</b> → <b>5b-exo</b>	<b>TS1bb</b>	98.36	154.17	-68.60
12	<b>1b+2b</b> → <b>6b-endo</b>	<b>TS2bb</b>	100.47	155.97	-66.38
13	<b>1b+2c</b> → <b>5c-exo</b>	<b>TS1bc</b>	64.58	120.92	-75.89
14	<b>1b+2c</b> → <b>6c-endo</b>	<b>TS2bc</b>	76.74	131.41	-71.40
15	<b>1b+2d</b> → <b>5d-exo</b>	<b>TS1bd</b>	108.51	162.17	-51.16
16	<b>1b+2d</b> → <b>6d-endo</b>	<b>TS2bd</b>	100.17	153.82	-54.83
17	<b>1c+2a</b> → <b>7a-exo</b>	<b>TS1ca</b>	94.23	151.39	-62.01
18	<b>1c+2a</b> → <b>8a-endo</b>	<b>TS2ca</b>	100.63	156.30	-59.89
19	<b>1c+2b</b> → <b>7b-exo</b>	<b>TS1cb</b>	98.40	153.68	-63.50
20	<b>1c+2b</b> → <b>8b-endo</b>	<b>TS2cb</b>	100.22	155.34	-59.66
21	<b>1c+2c</b> → <b>7c-exo</b>	<b>TS1cc</b>	91.26	148.47	-43.06
22	<b>1c+2c</b> → <b>8c-endo</b>	<b>TS2cc</b>	101.83	157.25	-41.22
23	<b>1c+2d</b> → <b>7d-exo</b>	<b>TS1cd</b>	106.23	160.32	-41.75
24	<b>1c+2d</b> → <b>8d-endo</b>	<b>TS2cd</b>	98.22	152.36	-45.00

ment with the non-polar character of these pathways. On the other hand, the *CT* values at the **TSs** of the DA reactions of **1a–c** and **2a–c** in the most favorable regioisomeric pathways (*meta-exo*), were between 0.205 and 0.157 e, which indicate the polar nature of the *meta* channels in these DA reactions. Only the most unfavorable DA reactions of **1a–c** and **2d** presented low *CT* values (lower than 0.050 e). These results with the proposal that for the DA reactions of **1a–c** with **2a–d**, an increase in the polar character as the reaction proceeds is accompanied by an acceleration of the reaction.<sup>7–9</sup>

The energy barrier ( $\Delta E^\ddagger$ ) and activation Gibbs free energy values ( $\Delta G^\ddagger$ ), related to the occurrence of transition states for the DA reactions of **1a–c** with **2a–d** are lower for the *meta* approaches than those for the *para* ones (Table I). The measured stereoselectivity indicated that the *meta-exo* cyclization modes are more favorable than the *meta-endo* ones, leading to the formation of *meta-exo* adducts for the DA reactions of **1a–c** with **2a–c**, while the lowest barrier energies for the DA reactions of **1a–c** with **2d** occur on the *meta-endo* pathway, which yields the *meta-endo* cycloadducts **4d**, **6d** and **8d**. Therefore, the presence of a cyano group

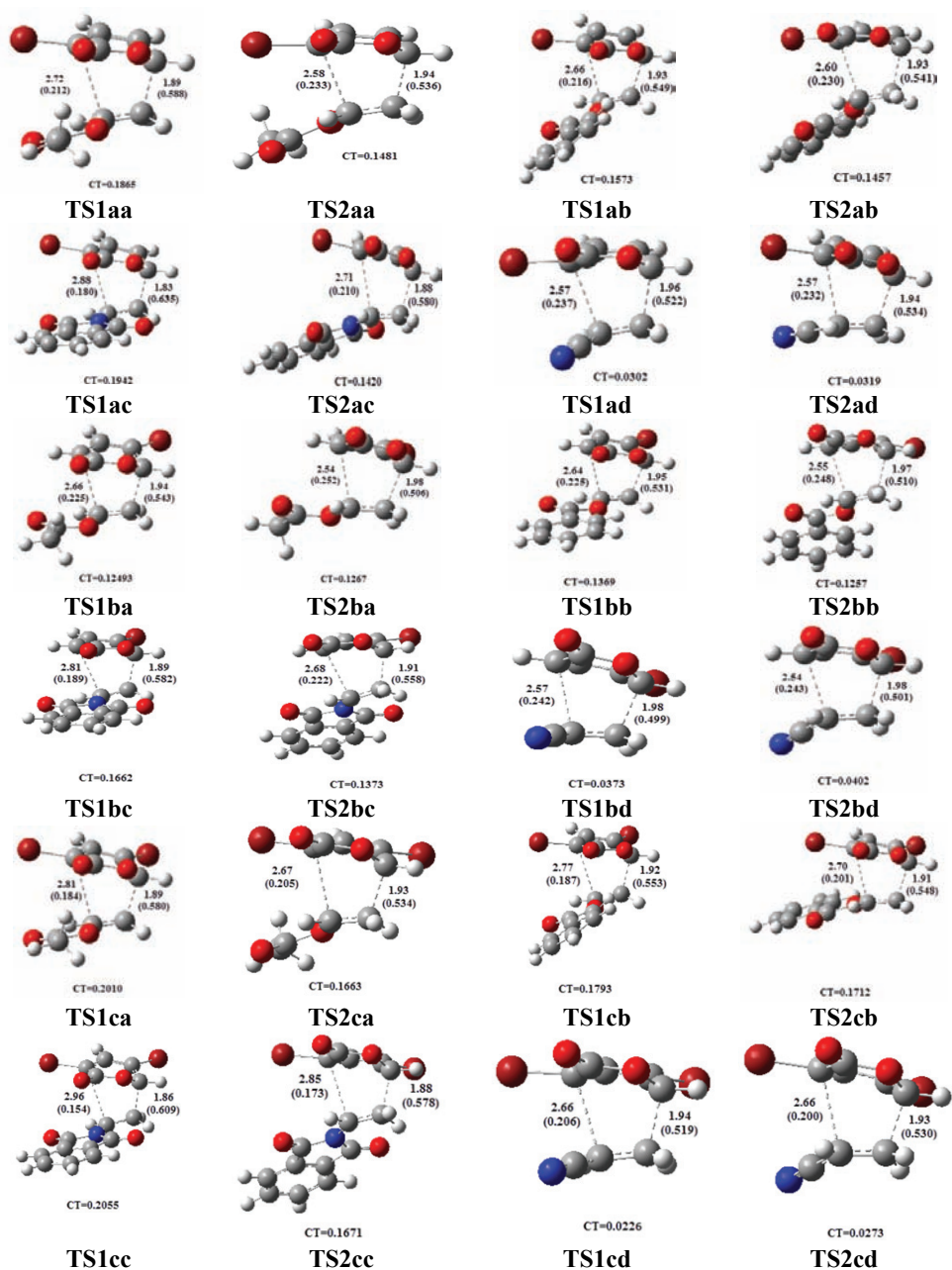


Fig. 1. Optimized geometries (B3LYP/cc-pVDZ) of the transition structures involved in the *meta* pathways of the DA reactions between the bromo-substituted 2*H*-pyran-2-ones **1a–c** and the vinyl derivatives **2a–d**. The bond distances are given in Å, the Wiberg bond indices are given in parenthesis and the natural charges (*CT*) of the TSs are also given.

on the dienophile, neither changes the stereoselectivity (*exo* to *endo*), nor increase the energy barriers relative to the other dienophiles.

On the other hand, the results of energy values in Table I showed that the DA reactions of **1a–c** with **2a** and **2b** are less stereoselective than the cycloadditions to dienophiles **2c** and **2d**. These differences in stereoselectivity could be explained as follows.

The lack of stereoselectivity in the cycloadditions of vinyl acetate **2a** presumably arises from a lack of strong secondary orbital interactions, suggesting that the cycloaddition to the weakly activated dienophile may be much more susceptible to steric interaction.<sup>7</sup> This was confirmed from the results of the cycloadditions of 2-ethenyl-1*H*-isoindole-1,3(2*H*)-dione (**2c**), where the reactions are highly *exo* selective. Here, the steric congestion arises directly from an unfavorable steric interaction between the second nitrogen substituent and the bromine atom in the **TS**, leading to the *endo* cycloadduct. Therefore, **TS1ac**, **TS1bc** and **TS1cc** leading to the *exo* cycloadduct are favored. This does not arise in the **TS** of *endo* cycloadduct of vinyl benzoate **2b** since the benzoate group can swing away from the bromine in the transition state. Moreover, the *endo* predomination in the cycloaddition of 2-propenenitrile (**2d**) is attributed to secondary orbital interactions and therefore it was not expected that cycloaddition to the bromo-2*H*-pyran-2-ones **1a–c** would give an *endo* to *exo* ratio of nearly one.

As can be seen in Table I and Scheme 1, it is possible to correlate the calculated energy of the transition state to the final yield of the cycloadducts **3–13**. The calculated values of all transition states confirmed that the ones likely to be the most abundant are the **3**, **5** and **7** isomers in all cases, which occurred in the DA reactions of **1a–c** with **2c**. The cycloadditions of **1a–c** with **2d** in all of reactions had the highest relative energy and it was expected to be the most disfavored cycloadduct.

The results of calculated free activation energies ( $\Delta G^\ddagger$ ) for DA reactions of 3,5-dibromo-2*H*-pyran-2-one (**1c**) with **2a**, **2b** and **2d** demonstrate the lowest activation free energy, while an increasing barrier energy has been seen for **1c** and **2c**. With considering FMO approach (Table II), broadly speaking, 3-bromo, 5-bromo and 3,5-dibromo-2*H*-pyran-2-one should undergo normal and inverse electron demand cycloadditions with dienophiles bearing weakly electron-donating (**1a–c**) and electron-withdrawing (**2d**) substituents, respectively.

#### DFT-based reactivity indices

The molecular DFT-based parameters, electronic chemical potential ( $\mu$ ), chemical hardness ( $\eta$ ), global electrophilicity ( $\omega$ ) and global nucleophilicity ( $N$ ) of the reactants **2a–d** and **1a–c** are displayed in Table II.

As can be seen in Table II, the bromo-2*H*-pyran-2-one derivatives **1a–c** are more electrophilic than the dienophiles **2a–d** and 3,5-dibromo-2*H*-pyran-2-one

(**1c**) with the highest electrophilicity ( $\omega = 2.43$  eV) being classified as a strong electrophile on the electrophilicity scale.<sup>20</sup> On the other hand, **1a** has a high nucleophilicity index,  $N = 2.52$  eV, and thus is classified as a strong nucleophile on the nucleophilicity scale.<sup>21</sup> This ambiphilic behavior is the consequence of the presence of the enone and oxygen atom inside **1a–c**. The electronic chemical potential ( $\mu$ ) of the bromo-2*H*-pyran-2-one derivatives **1a–c** are lower than those of the dienophiles, **2a** (−0.134), **2b** (−0.156) and **2c** (−0.130), indicating that charge transfer along the corresponding reactions will occur from the dienophiles **2a–c** to the electron deficient dienes **1a–c**. While as expected, a CN group (**2d**) decreases the chemical potential and increases the electrophilicity toward the dienophiles **2a–d**, and hence, these results are in agreement with the increase in the activation energy.

TABLE II. HOMO and LUMO energies, electronic chemical potential,  $\mu$ , chemical hardness,  $\eta$ , (all in a.u.), global electrophilicity,  $\omega$ , and nucleophilicity,  $N$  (both in eV), for the reactants obtained at the B3LYP/cc-pVDZ level of theory

Species	$E_{\text{HOMO}}$	$E_{\text{LUMO}}$	$\mu$	$\eta$	$\omega$	$N$
<b>1a</b>	−0.24366	−0.07747	−0.160	0.166	2.09	2.52
<b>1b</b>	−0.24586	−0.07990	−0.162	0.166	2.15	2.40
<b>1c</b>	−0.24777	−0.08881	−0.168	0.158	2.43	2.41
<b>2a</b>	−0.25309	−0.01470	−0.134	0.238	1.02	2.27
<b>2b</b>	−0.25205	−0.06044	−0.156	0.192	1.71	2.29
<b>2c</b>	−0.24195	−0.01862	−0.130	0.223	1.03	2.57
<b>2d</b>	−0.26633	−0.08384	−0.178	0.182	2.28	1.90

The polar character of a cycloaddition process can be predicted using the electrophilicity difference of the reaction pair,  $\Delta\omega$ .<sup>22</sup> In this sense, the electrophilicity differences between the diene **1c** and the dienophiles **2a** and **2c** are about 1.40, indicating a large polar character for these cycloadditions, while the small  $\Delta\omega$  between **1a** and **2b** (0.38 eV) and between **1b** and **2d** (0.21 eV) show a low polar character for these cycloaddition reactions. The Parr indices, local electrophilicity indices and local nucleophilicity indices for the atoms C6 and C3 of the pyrones **1a–c**, and C7 and C8 of the dienophiles **2a–d** are given in Table III (see Scheme 1 for atom numbering). The Parr functions (the electrophilic,  $P_k^+$ , and nucleophilic,  $P_k^-$ ) were computed based on Mulliken atomic spin density analysis.

According the Domingo model,<sup>15,17</sup> along a polar cycloaddition involving asymmetric reagents, the most favorable reactive channel is that involving the initial two-center interaction between the most electrophilic center ( $\omega_k$ ) at the electrophile and the most nucleophilic center ( $N_k$ ) at the nucleophile. According to this model, in the cycloaddition reactions of **1a–c** with dienophiles **2a–d**, the most favorable two-center interaction occurs between C6 of the dienes and C8 of



dienophiles **2a–d**, leading to the formation of the **3–13** regioisomers, which is in agreement with the experimental results.<sup>7–9</sup>

TABLE III. The Parr functions ( $P_k^-$ ,  $P_k^+$  / au), local electrophilicity indices ( $\omega_k$  / eV) and local nucleophilicity ( $N_k$  / eV) indices for the C6 and C3 atoms of the pyrones **1a–c** and for atoms C7 and C8 of the dienophiles at the reactive sites for the reactants obtained at the B3LYP/cc-pVDZ level of theory

Species	$k$	$P_k^-$	$P_k^+$	$N_k$	$\omega_k$
<b>1a</b>	C6	0.188	0.381	0.474	0.795
	C3	0.253	0.204	0.639	0.426
<b>1b</b>	C6	0.394	0.205	0.945	0.492
	C3	0.232	0.264	0.558	0.634
<b>1c</b>	C6	0.240	0.384	0.580	0.932
	C3	0.188	0.222	0.453	0.540
<b>2a</b>	C7	0.181	0.171	0.410	0.174
	C8	0.291	0.548	0.660	0.559
<b>2b</b>	C7	0.018	0.074	0.040	0.127
	C8	0.092	0.357	0.212	0.610
<b>2c</b>	C7	0.009	0.037	0.024	0.038
	C8	0.019	0.476	0.050	0.490
<b>2d</b>	C7	0.219	0.260	0.146	0.594
	C8	0.606	0.426	1.152	0.972

#### CONCLUSIONS

DFT computations using the B3LYP functional in conjunction with the cc-pVDZ basis set were used to analyze the outcome of the DA reactions of the bromo-2*H*-pyran-2-ones **1a–c** with some weakly activated and unactivated vinyls. The following conclusions could be inferred from the results of the energies:

I. The activation energies associated with the DA reaction of cyclic dienes **1a–c** with dienophile **2c** is more favorable than those for the reactions with **2a**, **b** and **2d**. The low reactivities of the dienophiles in these DA reactions correspond with their nucleophilic character.

II. While the DA reactions with **2a–c** are *exo* selective, the reaction with **2d** is *endo* selective.

III. 3,5-Dibromo-2*H*-pyran-2-one is more active than 3- and 5-bromo-2*H*-pyran-2-ones, having a lower energy barrier.

IV. These DA reactions proceed *via* a polar, regioselective and highly asynchronous process.

ИЗВОД  
ТЕОРИЈСКА СТУДИЈА ДИЛС–АЛДЕРОВЕ РЕАКЦИЈЕ БРОМО–СУПСТИТУИСАНИХ  
2H-ПИРАН-2-ОНА И НЕКИХ СУПСТИТУИСАНИХ ВИНИЛА

MINA HAGHDADI, HAMED AMANI и NASIM NAB

*Department of Chemistry, Islamic Azad University, P. O. Box 755, Babol branch, Babol, Iran*

Извршено је DFT испитивање реактивности, регио- и стереоселективности Дилс–Алдрове реакције између 3-бромо, 5-бромо и 3,5-дибромо-2H-пиран-2-она и неких слабо активираних и неактивираних алкена. Истражена су четири могућа реакциона пута, који обухватају формирање *меџа*-, *џара*-, *ендо*- и *еџо*-циклоадукта. Анализа заснована на енергији и природним орбиталама показује да је преферирана *меџа*-региоселективност и *еџо*-реакциони механизам.

(Примљено 5. децембра 2014, ревидирано 8. фебруара, прихваћено 8. фебруара 2015)

REFERENCES

1. K. Afarinkia, T. D. Nelson, M. V. Viader, G. H. Posner, *Tetrahedron* **48** (1992) 9111
2. B. T. Woodward, G. H. Posner, *Adv. Cycloaddit.* **5** (1999) 47
3. a) C.-G. Cho, Y.-W. Kim, Y.-K. Lim, J.-S. Park, H. Lee, S. Koo *J. Org. Chem.* **67** (2002) 290; b) C.-G. Cho, J.-S. Park, I.-H. Jung, H. Lee, *Tetrahedron Lett.* **42** (2001) 1065
4. G. H. Posner, T. D. Nelson, C. M. Kinter, K. Afarinkia, *Tetrahedron Lett.* **32** (1992) 5295
5. K. Afarinkia, G. H. Posner, *Tetrahedron Lett.* **33** (1992) 7839
6. G. H. Posner, K. Afarinkia, H. Dai, *Org. Synth.* **73** (1995) 231
7. K. Afarinkia, N. T. Daly, S. Gomez-Farnos, S. Joshi, *Tetrahedron Lett.* **83** (1997) 2369
8. K. Afarinkia, M. J. Bearpark, A. Ndibwami, *J. Org. Chem.* **70** (2005) 1122
9. K. Afarinkia, M. J. Bearpark, A. Ndibwami, *J. Org. Chem.* **68** (2003) 7158
10. Gaussian 09, Revision A, Gaussian, Inc., Wallingford, CT, 2009
11. A. E. Reed, R. B. Weinstock, F. Weinhold, *J. Chem. Phys.* **83** (1985) 735
12. R. G. Parr, R. G. Pearson, *J. Am. Chem. Soc.* **105** (1983) 7512
13. R. G. Parr, L. Von Szentpaly, S. Liu, *J. Am. Chem. Soc.* **121** (1999) 1922
14. R. G. Parr, W. Yang, *Density functional theory of atoms and molecules*, Oxford University Press, New York, 1989, p 16
15. L. R. Domingo, P. Pérez, *J. Org. Chem.* **73** (2008) 4615
16. L. R. Domingo, P. Pérez, J. A. Saez, *RSC Adv.* **3** (2013) 1486
17. L. R. Domingo, M. J. Aurell, P. Pérez, *J. Phys. Chem., A* **106** (2002) 6871
18. P. Pérez, L. R. Domingo, M. Duque-Noreña, E. Chamorro, *J. Mol. Struct.: THEOCHEM* **895** (2009) 86
19. K. B. Wiberg, *Tetrahedron* **24** (1968) 1083
20. L. R. Domingo, M. J. Aurell, P. Perez, R. Contreras, *Tetrahedron* **58** (2002) 4417
21. I. Kim, K. A. Hoff, E. T. Hessen, T. Haug-Warberg, H. F. Svendsen, *Chem. Eng. Sci.* **64** (2009) 2027
22. H. Chemouri, S. M. Mekelleche, *Int. J. Quantum Chem.* **112** (2012) 2294.